Constraining the Nature of Dark Matter Subhalos with Lensed Gravitational Waves

Luka Vujeva,[1,] Maddalena Reggio,[1,] Jose María Ezquiaga,[1] Maya Silverman,[2] and Sarah Pearson[3,2]

[1] *Center of Gravity, Niels Bohr Institute, Blegdamsvej 17, 2100 Copenhagen, Denmark*
[2] *DARK, Niels Bohr Institute, University of Copenhagen, Jagtvej 155A, 2200 Copenhagen, Denmark*
[3] *Technical University of Denmark, Elektrovej 327, 2800 Kgs. Lyngby, Denmark*

The nature of dark matter remains elusive. A key open question is how much it clumps at small scales, with recent observations finding high concentrations consistent with core-collapsed subhalos. In this *Letter*, we show that strongly lensed gravitational waves can discover or constrain such substructures, which would produce additional copies of the original signal and wave-optics features. We find that within 3 years of next-generation ground-based detectors one could distinguish self-interacting scenarios from cold and warm dark matter at ~ 3–5σ. Even with conservative rates, a single additional copy detected during 10 years of current observatories would disfavor cold dark matter at $> 2\sigma$. Finally, we report that those collapsed low mass subhalos produce a median of ~ 5 times greater wave-optics effects in future space-based detector's signals, further motivating the use of gravitational waves as a premier probe of the nature of dark matter at small scales.

Introduction.—When looking into the distant past, every cosmic messenger is sensitive to the distribution of matter in the Universe through gravitational lensing. In fact, this is how we collect some of the strongest evidence for the existence of dark matter (DM) [1]. However, the resolution at which we observe such lensed messengers determines the scale at which DM substructures can be resolved. Importantly, it is only at small scales where currently viable DM models differ from each other [2].

Electromagnetic observations of strongly lensed galaxies have proven a powerful DM probe [3] and, in recent times, even hint at deviations from the standard cold dark matter (CDM) scenario [4, 5]. If confirmed, such observations point to the existence of very compact subhalos, which could be consistent with predictions from self-interacting dark matter (SIDM) [6]. On the opposite end, strong lensing also constrains warm dark matter (WDM), which suppresses the halo mass function [7–9]. Nonetheless, such surveys are intrinsically limited by their angular resolution to subhalo masses $\gtrsim 10^6 M_\odot$. Alternative methods such as stellar streams or Milky Way satellite counts offer complementary bounds in the same mass range [10, 11].

In the landscape of probing DM substructures, gravitational waves (GWs) appear as a promising new messenger. GWs are coherently emitted and detected, with waveforms predicted from general relativity. Across cosmological propagation, these signals are only affected by gravitational lensing. The exquisite time resolution of current GW detectors [12–14], down to the millisecond, implies direct sensitivity to lens masses as low as $\sim 100 M_\odot$. On the opposite end, the year-long observing runs guarantees the observation of lensing signatures up to the largest galaxy clusters $\sim 10^{15} M_\odot$ [15, 16]. For masses up to $\sim 10^5 M_\odot$, GW lensing in ground-based detectors is characterized by waveform distortions, as the repeated copies produced by strong lensing interfere and diffract with each other [17]. For higher lens masses, multiple copies arrive at the detector at different times, with distinct characteristics that can trace substructures [15, 18–20].

Approximately 1 in every 1000 GWs from stellar-mass binaries is expected to be strongly lensed by galaxy-scale lenses and above [21–26]. This motivates current searches [27–29] and the exploration of DM tests with future observations [18, 19]. Because the limited detection reach of current GW observatories, strongly lensed signals are expected around regions of high-magnification [30], where substructure effects are boosted [18], and diffraction becomes relevant [31]. Importantly, any other astrophysical substructures such as globular clusters or intermediate-mass black holes are unlikely to produce observable effects in GWs due to their low abundances near regions of high-magnification [32]. Future space-based detectors such as LISA are also promising probes, with larger subhalos leading to wave-optics features [33–37].

Given the promise of GWs as precision probes of masses currently out of reach to electromagnetic observatories, in this *Letter*, we explore the constraining power that lensed binary black holes (BBHs) and binary neutron stars (BNSs) can have on the particle nature of DM. More specifically, we consider fiducial examples of the CDM, WDM, and SIDM paradigms, and quantify the distinctions we can make between instances of these models using current and next-generation detectors.

Modeling Dark Matter Subhalos.—The particle nature of DM extensively changes the properties of both the density profile of each DM subhalo, as well as their mass dependent number density [38]. In the standard CDM paradigm, the density profiles of DM subhalos are expected to follow the truncated Navarro-Frenk-White (TNFW) profile [39, 40], whose density distribution is

luka.vujeva@nbi.ku.dk
maddalena.reggio@nbi.ku.dk

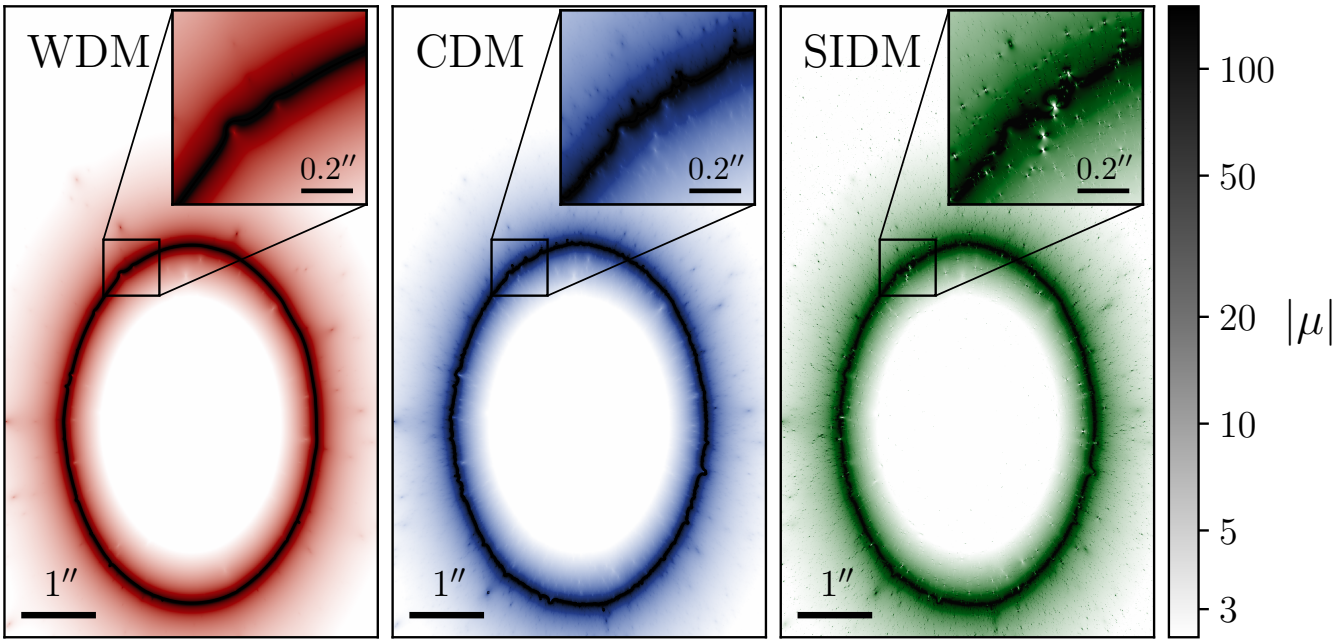


FIG. 1. Image plane magnification maps for a $10^{13} M_\odot$ main halo at $z_\mathrm{L} = 0.5$, and a source at $z_\mathrm{S} = 2$ in warm dark matter (WDM), cold dark matter (CDM) and self-interacting dark matter (SIDM), from left to right. Subhalos with $\leq 10^7 M_\odot$ in CDM/WDM produce small perturbations to the critical curves, whereas their core-collapsed equivalents in SIDM can produce meaningful perturbations, as seen by the abundance of small-scale structure in the critical curves in the SIDM panel. The SIDM example shown here is for the model with more collapsed subhalos consider in this work, SIDM100, with a viscosity cross section of $\sigma_\mathrm{v}/m = 100$ cm^{2}g^{-1}, to make the qualitative differences in the model clearly visible by eye.

controlled by a characteristic mass M, and concentration c, and truncation radius r_t. Thus, in our CDM models, subhalos are simply described by TNFW profiles [40], with concentrations following the $c-M$ relation of Diemer and Joyce [41]. For WDM, the free-streaming of DM particles suppresses both the abundance and concentrations of subhalos, particularly at low masses [42], while their profiles remain TNFW. This results in an under-abundance of WDM subhalos at low masses, as well as less concentrated subhalos overall given the delay in subhalo formation due to the free-streaming at early times. In this work, we follow the prescription of Ref. [43], and adopt a half-mode mass of $10^{7.5} M_\odot$.

DM self-interactions instead reshape the subhalos themselves, first forming isothermal cores [44] and, given sufficient time, undergoing gravothermal core collapse [45]. These subhalos are modeled with a cored truncated Navarro-Frenk-White (TNFWC) in order to capture the effects of the core formation. Throughout this work, DM self-interactions follow a velocity-dependent viscosity cross section $\sigma_\mathrm{v}(v)$ of the Rutherford-like form of Ref. [46]. To maximize the cross-section relevant for low-mass halos, which GWs are sensitive to, while remaining consistent with existing constraints [47, 48], we set the turnover velocity $w = 1\,\mathrm{km\,s^{-1}}$, while varying the characteristic cross-section, σ_0/m. Each model is labeled by its value at $v = 15\,\mathrm{km\,s^{-1}}$, namely $\sigma_\mathrm{v}/m = 10$, 50, and $100\,\mathrm{cm^2\,g^{-1}}$. Henceforth, we refer to these models as SIDM10, SIDM50, and SIDM100, respectively. Within this parametric model, increasing σ_0/m increases the collapse fraction of low-mass halos and increasing w increases the subhalo masses that undergo collapse. The core collapse timescale t_c of each subhalo then follows from its TNFWC parameters and velocity-averaged cross section [49].

The lensing observables are sensitive to how far this collapse is allowed to proceed, since subhalo cores become increasingly compact as it continues. In the parametric model of Ref. [49], each subhalo's evolution is tracked through the dimensionless time $\tau = t/t_\mathrm{c}$. While Ref. [49] stops the evolution of each halo at $\tau = 1$ to avoid extrapolating beyond the regime in which the model was calibrated, we find that this choice produces lensing observables indistinguishable to those of CDM for our simulated observables. Instead, we evolve subhalos to $\tau \leq 1.6$, using analytic extrapolations of the scale and core radii, which produces substantially denser central regions. Strong lensing analyses likewise model collapsed halos as deeply collapsed objects, with inner logarithmic slopes between -2 and -3 [50] or with profiles based on simulations that follow the collapse to $t/t_\mathrm{c} \sim 3$ [5, 51]. We also consider that tidal stripping accelerates core collapse in subhalos relative to isolated halos [52]. To account for this, we follow Ref. [50], measuring halo ages

from $z = 10$ and rescaling the subhalo collapse timescale as $t_{c,sub} = \gamma_{sub}\, t_c$, with $\gamma_{sub} = 0.4$.

Our choice is not intended to span the entire range of viable SIDM scenarios, nor to constrain them. Instead, it provides a representative example of a population of core-collapsed subhalos, which we use to illustrate the lensing signatures such a population can produce. How to model subhalos at late stages of collapse remains a key open systematic in SIDM lensing studies [50, 53]. Even within this simple framework, the collapse history of the population depends on choices such as the turnover velocity and normalization of the cross section, and on γ_{sub}, which sets how strongly tidal stripping accelerates collapse. Varying these quantities together leads to considerable degeneracies in the resulting subhalo population. Beyond this framework lies a much broader landscape of SIDM models with additional particle physics, such as inelastic [54] or dissipative self-interactions [55], which we do not consider here. We leave a systematic exploration of this parameter space, and of these alternative models, to future work.

The individual instances of the subhalo populations are generated using `pyHalo` [7]. In all cases, we consider a minimum mass of $10^5 M_\odot$, below which we find negligible contribution to the final results of this work. Finally, the subhalos are placed in a galaxy-scale lens, whose density distribution is given by an elliptical power law potential, which is characterized by a velocity dispersion, an axis ratio (taken to be 0.7 as a representative example), and a power law index, which was chosen to be 2, corresponding to an isothermal density distribution. The resulting image plane magnification maps for the three DM models are presented in Fig. 1.

Gravitational Wave Lensing with Dark Matter Subhalos.—Substructures in the potential of a galaxy introduce distinct observables in both the geometric optics (GO) and wave optics (WO) regimes. In GO, we have two main methods of inferring the existence of DM substructure: through the appearance of additional highly magnified images, and through the relative magnification (i.e. the absolute value of the brightest image's magnification divided by that of the second brightest image) of highly magnified events exceeding a value of 2 [18]. Due to the low redshift horizon of current detectors [56] and the steep increase with redshift of the optical depth, current (and near-future) ground-based detectors require relatively large magnifications, $\mu \gtrsim 5$, for detection [22, 57]. Since highly magnified images will inherently have shorter time delays [30, 58–60], current detectors will tend to detect pairs and triplets of images with shorter time delays [61, 62]. The increased sensitivity of future detectors will loosen this bias, capturing images produced by sources farther away from the caustic, as well as in the lower image multiplicity region outside of the main halo caustics that produces inherently lower magnifications, and longer time delays. In practice, a subhalo only alters images close to an existing image of the host, so we solve the smooth host (a singular isothermal ellipsoid with axis ratio 0.7) exactly and simulate subhalos only in small windows around individual host images: single images at fixed $|\mu|$ (minima, saddles and near-cusp images) and source boxes straddling a fold of the main caustic ($|\mu| \geq 10$), whose statistics each host image then inherits. In each window we solve the lens equation for the host plus every subhalo within three Einstein radii ($\mathcal{O}(10^5)$), summing those near the images ($\mathcal{O}(10^3)$) exactly and the rest through a Chebyshev interpolant of their combined deflection. Image po-

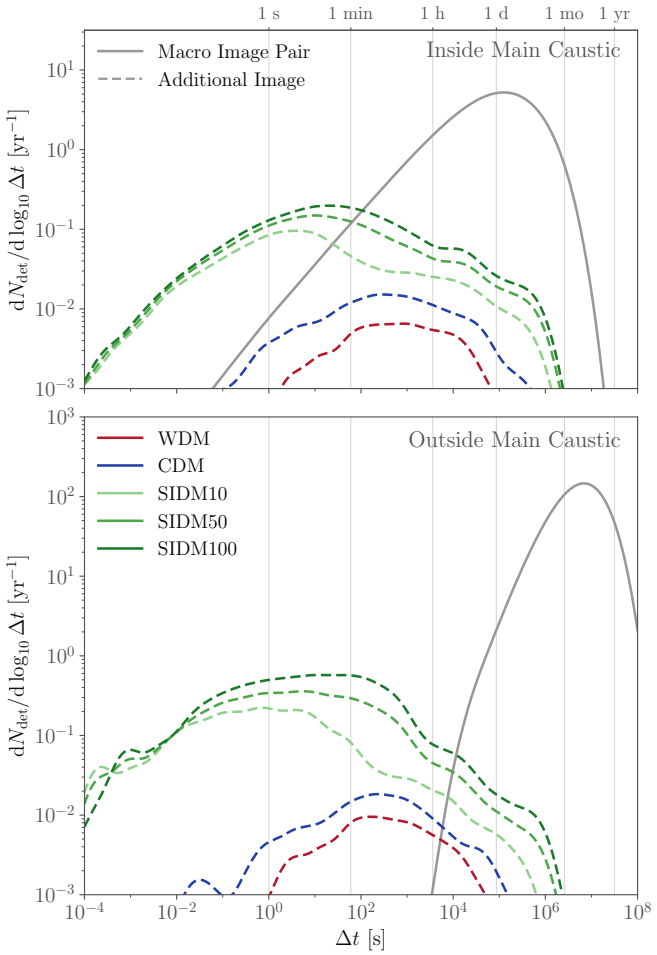


FIG. 2. Time delay distribution of the shortest detectable image pairs with ground-based detectors (Einstein Telescope) inside (top figure) and outside (bottom figure) of the perturbed main halo caustics for CDM, WDM and SIDM, for the optimistic merger rate. The production of additional structure in the caustics amplifies the high-magnification, and thus short time delay tail for sources inside the main caustics in the SIDM models (green lines). The core-collapsed halos' production of additional caustics outside those of the main halos produces a much more pronounced population of short time delay image pairs coming from the region outside of the main caustics, which in a smooth lens model, can generally only produce longer time delay pairs.

sitions, magnifications and time delays agree with the full `lenstronomy` [63] model to 10^{-8} arcsec, 10^{-5} and 10^{-5}, respectively, at more than 10^3 times lower cost. An event has an additional image when a host image splits into three or more images and the second brightest of that group (the third, for a fold pair) is detected; $R = |\mu_1/\mu_2|$ is computed from the two brightest images of the group. For each of the host masses and dark matter models, we use 300 subhalo populations (20 at each of 15 lens redshifts up to $z_l = 3$), each lensing 200 sources per source redshift out to $z_s = 20$, giving more than 10^5 lens simulations in total.

The time delay distribution of the shortest detectable image pair provides valuable insights, as seen in Fig. 2. For source positions *inside* the main caustic, SIDM subhalos enhance the short time delay tail below arrival time differences of 10 seconds. (corresponding to an effective lens mass of $\sim 10^6 M_\odot$). This enhancement is much more significant than in CDM, and almost non-existent in WDM. There, the short time delay tail is well below what is predicted by a smooth lensing potential (solid line). We have verified that the tail is preserved when the minimum subhalo mass is increased to $10^6 M_\odot$ the shape of the tail is preserved, while when increasing it to $10^7 M_\odot$, it disappears. At the other end, lowering the minimum mass to $10^4 M_\odot$ does not change the break point or enhancement, indicating that it is the $10^6 M_\odot$ halos which dominate the effect. For sources *outside* the main caustic, short time delays are solely produced by the subhalos, with SIDM again boosting the rate compared to CDM and WDM. In fact, with future ground-based detectors, most of the new detectable images lie outside the main caustic, as shown in Fig. 2. This is due to their increased sensitivity to images with lower magnifications, which dominate the cross section of strong lensing. In contrast, new signals in current detectors are dominated by subhalos within the main caustic, where SIDM still exceeds CDM, but by a lesser amount. For comparison, with current detectors, typical BBHs last for up to ∼seconds in band, while BNSs were observed for more than a minute. Therefore, the repeated new copies produced by subhalos could lead to overlapping GWs [64].

In the WO regime, we solve the diffraction integral numerically using `GLoW` [65, 66]. We quantify the effect of subhalos by computing the frequency dependent variations of the diffraction integral compared to a case without them (i.e. the maximum of $|F(f)/F_{\rm smooth}(f) - 1|$ across the band, normalized at its highest frequency so that the achromatic change in magnification is removed). For ground-based detector sources, defined as $f_{\rm min} > 10$Hz, we find that the Fresnel region is so small, $r_{\rm F} \simeq [cD_{\rm l}D_{\rm ls}/(\pi(1+z_{\rm l})D_{\rm s} f|\lambda|)]^{1/2} \approx 0.4\,{\rm pc}\,(f/10\,{\rm Hz})^{-1/2}|\lambda|^{-1/2}$ (i.e. ~ 1 pc for a typical image with $\mu \sim 5$), that the number density of subhalos is not high enough to give an effect: on average only $\sim 10^{-2}$ subhalos above $10^3 M_\odot$ fall within it, and the typical image varies by $\lesssim 10^{-4}$ in $|F|$ (mismatches $\lesssim 10^{-7}$). Only rare close encounters ($\lesssim 1$ percent of images) with collapsed SIDM subhalos produce $\sim 10\%$ features. For space-based detector sources, defined as $10^{-3} \leq f \leq 10^{-1}$Hz, we find variations of $\sim 0.6\%$ in CDM (0.2–2 percent across the 5th–95th percentiles), in agreement with [35]. When moving to SIDM, these effects are boosted by a median of ∼5–6 times, with SIDM exceeding CDM in 96% of sight-lines. On the contrary, WDM leads to negligible WO features. We do not consider the effects of lens stochastic diffraction that may be extracted in a population level analysis [67].

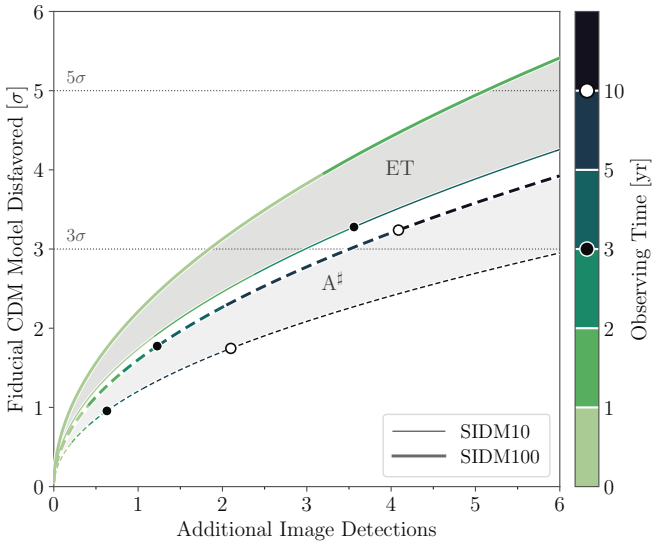


FIG. 3. The significance at which our fiducial CDM model would be disfavored given the additional new detectable images produced by SIDM subhalos, shown for our lowest and highest viscosity cross sections SIDM10, and SIDM100, with thin and thick lines respectively. We forecast constraints for LIGO's planned upgrade (A$^\sharp$, dashed) and next-generation detector Einstein Telescope (ET, solid) for an optimistic BBH merger rate consistent with GWTC-5. The color bar tracks the observing time, with the filled and unfilled black circles highlighting 3 and 10 years.

Constraints on dark matter.—The presence of compact DM subhalos leaves distinct signatures in strongly lensed GWs. Naturally, the (non)observation of such effect allows us to constrain the underlying DM model. For SIDM, we control the fraction of core-collapsed halos through the viscosity cross section over mass, $\sigma_{\rm V}/m$, which we vary from 10 to 100 cm^2/g vary the fraction of collapsed low-mass subhalos. A larger $\sigma_{\rm V}/m$, results in more higher mass subhalos collapsing. As a consequence, we observe that all the observable properties of subhalo lensing (high image multiplicity, large relative magnifications, short time delays and wave-optics features) increase with $\sigma_{\rm V}/m$. In order to forecast constraints on SIDM with ground-based detectors, we consider a population of stellar-mass compact

objects (BBHs and BNSs) as sources, whose properties are consistent with the latest observations from LIGO–Virgo–KAGRA (LVK) [68] and whose merger rate is extrapolated at high redshift to follow the star formation rate [69]. We also assume standard distributions for the main halos, which are drawn from a Schechter function fitted to the observations of the Sloan Digital Sky Survey [70], for galaxy masses of $10^{10} - 10^{13} M_\odot$ at redshifts of $z_{\rm L} \in [0.1, 3.0]$. Sources are placed behind each simulated lens at $z_{\rm S} \in [z_{\rm L} + 0.1, 20.0]$. We consider different ground-based detector configurations ranging from LVK at present sensitivity (O4), design sensitivity (O5) [71], LIGO's planned upgrade (A$^\sharp$) [72, 73], and next-generation detector Einstein Telescope (ET) [74]. Similar results hold for Cosmic Explorer [75].

We find that current detectors are similarly sensitive to the effects of subhalos in high-magnification regions as future detectors. Therefore, the first strongly lensed GW observations with LVK are proportionally more likely to have additional images from subhalos, ranging from 4.1% to 6.5%, from SIDM10 to SIDM100 respectively. For reference, our fiducial CDM model predicts 1.5%. With improved sensitivity in the detectors, more strongly lensed GWs are detected in general. The gain in subhalo signatures is not proportional, as these events typically come from regions with lower magnifications: from present O4 sensitivity to ET the strongly lensed rate grows by a factor of ∼600, the additional-image rate by only ∼60–100, and the fraction falls to 0.4–1 %. Importantly, we find that in ∼45% of cases the new detectable copies in O5 have time delays shorter than 1 second, potentially leading to overlapping signals.

Figure 3 summarizes how well A$^\sharp$ and ET can distinguish between DM models. As only a small fraction of lensed events produce additional images, this constraining power depends strongly on the GW merger rate, particularly at high redshifts where lensing is most efficient. We stress that these constraints apply only to our fiducial CDM and WDM models described above, rather than to these paradigms in general. With optimistic merger rates, ET could discern our fiducial CDM model from SIDM, even for the mildest cross section (SIDM10), at 3σ within 2.5 years, and from SIDM100 at 5σ within only 1.6 years. Even A$^\sharp$ could see first hints of SIDM subhalos after ten years of observations, differentiating our fiducial CDM model at 1.7, 3.2σ from SIDM10 and SIDM100 respectively. With conservative merger rates, constraints become much harder to obtain: after ten years of ET observations, our fiducial CDM model could be distinguished at only 3.4σ, even for the largest cross section, SIDM100. Our fiducial WDM model, in contrast, predicts additional-image rates approximately half that of CDM, and thus remains indistinguishable from it on these timescales using the additional detectable image probe considered in this work.

Based on current merger rates [76], we find that strongly lensed BNSs are unlikely until next-generation detectors. To be observable by current detectors, very high magnifications are required, $\mu \gtrsim 100$ [25]. We find that such detections are more likely to be affected by subhalos, with a probability that rises to 25-30%.

Conclusions.— The nature of DM is still elusive and the key to discern between different paradigms could lie in the small scale cosmological structures. We demonstrate that strongly lensed GWs are sensitive to DM subhalos, with effects growing rapidly with their compactness. Even if DM only self-interacts with the viscosity cross section of SIDM10, future ground-based detectors could disfavor our fiducial CDM model at 3σ within 2.5 years for optimistic merger rates, while SIDM100 would allow it to be excluded at 5σ within only 1.6 years. Even A$^\sharp$ could see first hints of SIDM subhalos after ten years of observations. With conservative merger rates, ten years of observations would disfavor our fiducial CDM and WDM models at only $\sim 3\sigma$ and $\sim 4\sigma$, respectively, even for the largest cross section.

The existence of core-collapsed subhalos in SIDM-like scenarios predicts enhanced WO signatures in the GWs detected by LISA [33, 34, 77]. There, the richness of the frequency dependent waveform distortions could bring new insights into the density profile of such subhalos. Additional work is needed, however, into solving and characterizing these diffraction patterns, as well as implementing them in search pipelines [78–80]. In future work, we will explore the broader range of SIDM models, from alternative cross sections and collapse prescriptions, to additional dark-sector physics [6, 81], and how these choices affect the lensing observables and the constraints they place on SIDM. Similarly, more work is required to discern the impact of DM subhalos for multi-messenger lensing searches [82], as we have found large probabilities of additional images in highly magnified BNSs. In those high-magnification cases, stellar fields could also contribute with additional distortions [83, 84].

While detailed modeling of the cosmic formation history of DM subhalos still needs to be accounted for, as well as the uncertainties in the merger rate of compact binaries that propagate into the lensing rates, our work shows that strongly lensed GWs are unique probes of DM substructures and can constrain the amount of core-collapsed subhalos, favoring or ruling out competing DM scenarios.

Acknowledgments.—We are grateful to Mark Cheung for useful conversations, and to Sreekanth Harikumar for reviewing the paper internally in LVK. Claude Opus 5.5 was used to assist in coding and verifying grammar in the manuscript. LV carefully reviewed all of Claude's outputs and takes full responsibility for all code used in this work. All scientific conclusions are the authors' own. This work was supported by Research Grants No. VIL37766 and No. VIL53101 from Villum Fonden and the DNRF Chair Program Grant

No. DNRF162 by the Danish National Research Foundation. J. M. E is also supported by the Marie Sklodowska-Curie Grant Agreement No. 847523 INTERACTIONS. The Center of Gravity is a Center of Excellence funded by the Danish National Research Foundation under grant no. DNRF184. This project has received funding from the European Union's Horizon 2020 research and innovation programme under the Marie Sklodowska-Curie grant agreement No 101299389 and No 101131233. This work is supported by Simons Foundation International [85] and the Simons Foundation [86] through Simons Foundation grant SFI-MPS-BH-00012593-11. MS and SP were supported by a research grant (VIL53081) from VILLUM FONDEN. Co-funded by the European Union (ERC, BeyondSTREAMS, 101115754). Views and opinions expressed are however those of the author(s) only and do not necessarily reflect those of the European Union or the European Research Council. Neither the European Union nor the granting authority can be held responsible for them. The Tycho supercomputer hosted at the SCIENCE HPC center at the University of Copenhagen was used for supporting this work. The authors also acknowledge the use of the Sophia workstation for this work.

[1] D. Clowe, M. Bradac, A. H. Gonzalez, M. Markevitch, S. W. Randall, C. Jones, and D. Zaritsky, A direct empirical proof of the existence of dark matter, Astrophys. J. Lett. **648**, L109 (2006), arXiv:astro-ph/0608407.

[2] J. S. Bullock and M. Boylan-Kolchin, Small-Scale Challenges to the ΛCDM Paradigm, Ann. Rev. Astron. Astrophys. **55**, 343 (2017), arXiv:1707.04256 [astro-ph.CO].

[3] S. Vegetti *et al.*, Strong Gravitational Lensing as a Probe of Dark Matter, Space Sci. Rev. **220**, 58 (2024), arXiv:2306.11781 [astro-ph.CO].

[4] P. Natarajan, B. T. Chiang, and I. Dutra, New Cold Dark Matter Crisis Revealed by Multiscale Cluster Lensing, Astrophys. J. Lett. **1001**, L12 (2026), arXiv:2601.07909 [astro-ph.CO].

[5] D. Gilman *et al.*, JWST lensed quasar dark matter survey V: Hints of self-interacting dark matter from 29 quadruply imaged quasars, (2026), arXiv:2609.35974 [astro-ph.CO].

[6] S. Adhikari *et al.*, Astrophysical tests of dark matter self-interactions, Rev. Mod. Phys. **97**, 045004 (2025), arXiv:2207.10638 [astro-ph.CO].

[7] D. Gilman, S. Birrer, A. Nierenberg, T. Treu, X. Du, and A. Benson, Warm dark matter chills out: constraints on the halo mass function and the free-streaming length of dark matter with eight quadruple-image strong gravitational lenses, Mon. Not. Roy. Astron. Soc. **491**, 6077 (2020), arXiv:1908.06983 [astro-ph.CO].

[8] E. O. Nadler, S. Birrer, D. Gilman, R. H. Wechsler, X. Du, A. Benson, A. M. Nierenberg, and T. Treu, Dark Matter Constraints from a Unified Analysis of Strong Gravitational Lenses and Milky Way Satellite Galaxies, Astrophys. J. **917**, 7 (2021), arXiv:2101.07810 [astro-ph.CO].

[9] R. E. Keeley *et al.*, JWST lensed quasar dark matter survey – II. Strongest gravitational lensing limit on the dark matter free streaming length to date, Mon. Not. Roy. Astron. Soc. **535**, 1652 (2024), arXiv:2405.01620 [astro-ph.CO].

[10] N. Banik, J. Bovy, G. Bertone, D. Erkal, and T. J. L. de Boer, Novel constraints on the particle nature of dark matter from stellar streams, JCAP **10**, 043, arXiv:1911.02663 [astro-ph.GA].

[11] E. O. Nadler *et al.* (DES), Milky Way Satellite Census. III. Constraints on Dark Matter Properties from Observations of Milky Way Satellite Galaxies, Phys. Rev. Lett. **126**, 091101 (2021), arXiv:2008.00022 [astro-ph.CO].

[12] J. Aasi *et al.* (LIGO Scientific), Advanced LIGO, Class. Quant. Grav. **32**, 074001 (2015), arXiv:1411.4547 [gr-qc].

[13] F. Acernese *et al.* (VIRGO), Advanced Virgo: a second-generation interferometric gravitational wave detector, Class. Quant. Grav. **32**, 024001 (2015), arXiv:1408.3978 [gr-qc].

[14] T. Akutsu *et al.* (KAGRA), Overview of KAGRA: Detector design and construction history, PTEP **2021**, 05A101 (2021), arXiv:2005.05574 [physics.ins-det].

[15] L. Vujeva, J. M. Ezquiaga, R. K. L. Lo, and J. C. L. Chan, Effects of galaxy cluster structure on lensed gravitational waves, Phys. Rev. D **112**, 063044 (2025), arXiv:2501.02096 [astro-ph.CO].

[16] X. Shan, Y.-F. Wang, S. Mao, H. Yang, and M. Zumalacárregui, Gravitational lensing of gravitational waves by galaxy clusters, (2026), arXiv:2609.16891 [astro-ph.GA].

[17] R. Takahashi and T. Nakamura, Wave effects in gravitational lensing of gravitational waves from chirping binaries, Astrophys. J. **595**, 1039 (2003), arXiv:astro-ph/0305055.

[18] L. Vujeva, J. M. Ezquiaga, D. Gilman, S. Goyal, and M. Zumalacárregui, Dark Matter Subhalos and Higher Order Catastrophes in Gravitational Wave Lensing, (2025), arXiv:2510.14953 [astro-ph.CO].

[19] T. Liu, K. Liao, M. Biesiada, and B. Sun, Gravitational-Wave Image Multiplicity as a Topological Probe of Dark-Matter Core Collapse, (2026), arXiv:2609.15462 [astro-ph.CO].

[20] I. Swamy, A. More, and O. Patil, Impact on time delays due to milli-lensing by subhalos on lensed gravitational waves, (2026), arXiv:2609.23428 [astro-ph.CO].

[21] K. K. Y. Ng, K. W. K. Wong, T. Broadhurst, and T. G. F. Li, Precise LIGO Lensing Rate Predictions for Binary Black Holes, Phys. Rev. D **97**, 023012 (2018), arXiv:1703.06319 [astro-ph.CO].

[22] M. Oguri, Effect of gravitational lensing on the distribution of gravitational waves from distant binary black hole mergers, Mon. Not. Roy. Astron. Soc. **480**, 3842 (2018), arXiv:1807.02584 [astro-ph.CO].

[23] F. Xu, J. M. Ezquiaga, and D. E. Holz, Please Repeat: Strong Lensing of Gravitational Waves as a Probe of Compact Binary and Galaxy Populations, Astrophys. J. **929**, 9 (2022), arXiv:2105.14390 [astro-ph.CO].

[24] A. R. A. C. Wierda, E. Wempe, O. A. Hannuksela, L. e. V. E. Koopmans, and C. Van Den Broeck, Beyond the Detector Horizon: Forecasting Gravitational-Wave Strong Lensing, Astrophys. J. **921**, 154 (2021), arXiv:2106.06303 [astro-ph.HE].

[25] G. P. Smith, A. Robertson, G. Mahler, M. Nicholl, D. Ryczanowski, M. Bianconi, K. Sharon, R. Massey,

J. Richard, and M. Jauzac, Discovering gravitationally lensed gravitational waves: predicted rates, candidate selection, and localization with the Vera Rubin Observatory, Mon. Not. Roy. Astron. Soc. **520**, 702 (2023), arXiv:2204.12977 [astro-ph.HE].

[26] Y. Li, K. Liao, M. Sun, L. Yang, X. Ding, M. Biesiada, and T. Liu, Mock Catalogs of Strongly Lensed Gravitational Waves via a Halo Model Approach with Ground-based Detectors, Astrophys. J. Suppl. **284**, 56 (2026), arXiv:2603.09289 [astro-ph.CO].

[27] R. Abbott *et al.* (LIGO Scientific, VIRGO), Search for Lensing Signatures in the Gravitational-Wave Observations from the First Half of LIGO–Virgo's Third Observing Run, Astrophys. J. **923**, 14 (2021), arXiv:2105.06384 [gr-qc].

[28] R. Abbott *et al.* (LIGO Scientific, VIRGO, KAGRA), Search for gravitational-lensing signatures in the full third observing run of the LIGO-Virgo network, (2023), arXiv:2304.08393 [gr-qc].

[29] A. G. Abac *et al.* (LIGO Scientific, VIRGO, KAGRA), GWTC-4.0: Searches for Gravitational-Wave Lensing Signatures, (2025), arXiv:2512.16347 [gr-qc].

[30] R. K. L. Lo, L. Vujeva, J. M. Ezquiaga, and J. C. L. Chan, Observational Signatures of Highly Magnified Gravitational Waves from Compact Binary Coalescence, Phys. Rev. Lett. **134**, 151401 (2025), arXiv:2407.17547 [gr-qc].

[31] J. M. Ezquiaga, R. K. L. Lo, and L. Vujeva, Diffraction around caustics in gravitational wave lensing, Phys. Rev. D **112**, 043544 (2025), arXiv:2503.22648 [gr-qc].

[32] L. Vujeva, J. M. Ezquiaga, R. K. L. Lo, and L. Zwick, Probability of gravitational-wave lensing by intermediate-mass black holes and globular clusters, (2026), arXiv:2608.07667 [astro-ph.CO].

[33] G. Tambalo, M. Zumalacárregui, L. Dai, and M. H.-Y. Cheung, Gravitational wave lensing as a probe of halo properties and dark matter, Phys. Rev. D **108**, 103529 (2023), arXiv:2212.11960 [astro-ph.CO].

[34] M. Çalışkan, N. Anil Kumar, L. Ji, J. M. Ezquiaga, R. Cotesta, E. Berti, and M. Kamionkowski, Probing wave-optics effects and low-mass dark matter halos with lensing of gravitational waves from massive black holes, Phys. Rev. D **108**, 123543 (2023), arXiv:2307.06990 [astro-ph.CO].

[35] S. Ando, Wave-Optics Imprints of Dark Matter Subhalos on Strongly Lensed Gravitational Waves, (2026), arXiv:2603.04267 [astro-ph.CO].

[36] S. Ando, Wave-optics imprints of dark matter subhalos on strongly lensed gravitational waves. II. Saddle images and detectability, (2026), arXiv:2606.21519 [astro-ph.CO].

[37] B. A. Thakore and S. Ando, Wave-Optics Imprints of Warm Dark Matter Subhalos with Prompt Cusps on Strongly Lensed Gravitational Waves, (2026), arXiv:2609.28626 [astro-ph.CO].

[38] E. O. Nadler, K. K. Rogers, and A. Drlica-Wagner, Dark Matter Constraints from Small-Scale Cosmic Structure (2026), arXiv:2607.28564 [astro-ph.CO].

[39] J. F. Navarro, C. S. Frenk, and S. D. M. White, The Structure of cold dark matter halos, Astrophys. J. **462**, 563 (1996), arXiv:astro-ph/9508025.

[40] J. F. Navarro, C. S. Frenk, and S. D. M. White, A Universal Density Profile from Hierarchical Clustering, Astrophys. J. **490**, 493 (1997), astro-ph/9611107.

[41] B. Diemer and M. Joyce, An accurate physical model for halo concentrations, Astrophys. J. **871**, 168 (2019), arXiv:1809.07326 [astro-ph.CO].

[42] M. Viel, G. D. Becker, J. S. Bolton, and M. G. Haehnelt, Warm dark matter as a solution to the small scale crisis: New constraints from high redshift Lyman-α forest data, Phys. Rev. D **88**, 043502 (2013), arXiv:1306.2314 [astro-ph.CO].

[43] A. J. Benson, E. O. Nadler, X. Du, and V. Gluscevic, A Unified Halo Mass Function Across Dark Matter Models from High-Resolution Multi-Scale Simulations, (2026), arXiv:2606.12137 [astro-ph.CO].

[44] D. N. Spergel and P. J. Steinhardt, Observational evidence for selfinteracting cold dark matter, Phys. Rev. Lett. **84**, 3760 (2000), arXiv:astro-ph/9909386.

[45] S. Balberg, S. L. Shapiro, and S. Inagaki, Selfinteracting dark matter halos and the gravothermal catastrophe, Astrophys. J. **568**, 475 (2002), arXiv:astro-ph/0110561.

[46] D. Yang and H.-B. Yu, Gravothermal evolution of dark matter halos with differential elastic scattering, Journal of Cosmology and Astroparticle Physics **2022** (09), 077, arXiv:2205.03392 [astro-ph.CO].

[47] C. A. Correa, Constraining velocity-dependent self-interacting dark matter with the Milky Way's dwarf spheroidal galaxies, Mon. Not. Roy. Astron. Soc. **503**, 920 (2021), arXiv:2007.02958 [astro-ph.GA].

[48] K. E. Andrade, J. Fuson, S. Gad-Nasr, D. Kong, Q. Minor, M. G. Roberts, and M. Kaplinghat, A Stringent Upper Limit on Dark Matter Self-Interaction Cross Section from Cluster Strong Lensing, Monthly Notices of the Royal Astronomical Society **510**, 54 (2021), arXiv:2012.06611 [astro-ph.CO].

[49] D. Yang, E. O. Nadler, H.-B. Yu, and Y.-M. Zhong, A parametric model for self-interacting dark matter halos, JCAP **02**, 032, arXiv:2305.16176 [astro-ph.CO].

[50] D. Gilman, Y.-M. Zhong, and J. Bovy, Constraining resonant dark matter self-interactions with strong gravitational lenses, Phys. Rev. D **107**, 103008 (2023), arXiv:2207.13111 [astro-ph.CO].

[51] J. Gurian and S. May, Core Collapse Beyond the Fluid Approximation: The Late Evolution of Self-Interacting Dark Matter Halos, Phys. Rev. Lett. **135**, 221001 (2025), arXiv:2505.15903 [astro-ph.CO].

[52] H. Nishikawa, K. K. Boddy, and M. Kaplinghat, Accelerated core collapse in tidally stripped self-interacting dark matter halos, Phys. Rev. D **101**, 063009 (2020), arXiv:1901.00499 [astro-ph.GA].

[53] D. Yang, E. O. Nadler, and H.-B. Yu, Testing the parametric model for self-interacting dark matter using matched halos in cosmological simulations, Phys. Dark Univ. **47**, 101807 (2025), arXiv:2406.10753 [astro-ph.CO].

[54] M. Vogelsberger, J. Zavala, K. Schutz, and T. R. Slatyer, Evaporating the Milky Way halo and its satellites with inelastic self-interacting dark matter, Monthly Notices of the Royal Astronomical Society **484**, 5437 (2019), aDS Bibcode: 2019MNRAS.484.5437V.

[55] S. Roy, X. Shen, J. Barron, M. Lisanti, D. Curtin, N. Murray, and P. F. Hopkins, Aggressively-Dissipative Dark Dwarfs: The Effects of Atomic Dark Matter on the Inner Densities of Isolated Dwarf Galaxies (2024), arXiv:2408.15317 [astro-ph.GA].

[56] A. G. Abac *et al.* (LIGO Scientific, VIRGO, KAGRA), GWTC-5.0: An Introduction to Version 5.0 of the Gravitational-Wave Transient Catalog, (2026),

arXiv:2605.27223 [gr-qc].
[57] A. Robertson, G. P. Smith, R. Massey, V. Eke, M. Jauzac, M. Bianconi, and D. Ryczanowski, What does strong gravitational lensing? The mass and redshift distribution of high-magnification lenses, Mon. Not. Roy. Astron. Soc. **495**, 3727 (2020), arXiv:2002.01479 [astro-ph.CO].
[58] P. Schneider, J. Ehlers, and E. E. Falco, *Gravitational Lenses* (1992).
[59] T. Baka, H. Narola, J. Janquart, A. Samajdar, T. Dietrich, and C. Van Den Broeck, Overlapping signals in next-generation gravitational wave observatories: A recipe for selecting the best parameter estimation technique, Phys. Rev. D **112**, 082001 (2025), arXiv:2507.10304 [gr-qc].
[60] N. Rao, A. Mishra, A. Ganguly, and A. More, Comprehensive analysis of time-domain overlapping gravitational wave transients: A lensing study, Phys. Rev. D **113**, 023054 (2026), arXiv:2510.17787 [gr-qc].
[61] K. Haris, A. K. Mehta, S. Kumar, T. Venumadhav, and P. Ajith, Identifying strongly lensed gravitational wave signals from binary black hole mergers, (2018), arXiv:1807.07062 [gr-qc].
[62] A. More and S. More, Improved statistic to identify strongly lensed gravitational wave events, Mon. Not. Roy. Astron. Soc. **515**, 1044 (2022), arXiv:2111.03091 [astro-ph.CO].
[63] S. Birrer and A. Amara, Lenstronomy: multi-purpose gravitational lens modelling software package 10.1016/j.dark.2018.11.002 (2018), arXiv:1803.09746 [astro-ph.CO].
[64] Recent studies have claimed to have not found additional images formed by CDM subhalos [20]. However, this appears to be due to insufficient sampling of the source plane. Our rate of additional image formation in CDM is substantially lower than their 200 simulated events.
[65] H. Villarrubia-Rojo, S. Savastano, M. Zumalacárregui, L. Choi, S. Goyal, L. Dai, and G. Tambalo, Gravitational lensing of waves: Novel methods for wave-optics phenomena, Phys. Rev. D **111**, 103539 (2025), arXiv:2409.04606 [gr-qc].
[66] GLoW: Gravitational lensing of waves, `https://github.com/glow-astro/GLoW`, accessed 2026-11-17.
[67] H. G. Choi, J. Urrutia, and M. Zumalacárregui, Signatures of $10 - 10^4\,\mathrm{M}_\odot$ Dark Matter halos in LISA via Stochastic Diffraction, (2026), arXiv:2607.11887 [astro-ph.CO].
[68] A. G. Abac *et al.* (LIGO Scientific, VIRGO, KAGRA), GWTC-5.0: Population Properties of Merging Compact Binaries, (2026), arXiv:2605.27226 [astro-ph.HE].
[69] More specifically, we choose values of the merger-rate density $\mathcal{R}(z) \propto (1+z)^{\alpha_z}/[1+((1+z)/(1+z_p))^{\alpha_z+\beta_z}]$ with a local rate at the upper end of the GWTC-5 90% interval, $\mathcal{R}(z=0.2) = 36.85\,\mathrm{Gpc}^{-3}\,\mathrm{yr}^{-1}$, and a redshift evolution that peaks later and falls off more slowly ($\alpha_z = 3.2$, $z_p = 3$, $\beta_z = 2.25$) than the GWTC-5 fiducial model [68] ($\mathcal{R}(z=0.2) = 30.4\,\mathrm{Gpc}^{-3}\,\mathrm{yr}^{-1}$, $\alpha_z = 2.54$, $z_p = 1.9$, $\beta_z = 3.06$).
[70] Y.-Y. Choi, C. Park, and M. S. Vogeley, Internal and Collective Properties of Galaxies in the Sloan Digital Sky Survey, Astrophys. J. **658**, 884 (2007), arXiv:astro-ph/0611607.
[71] LVK Collaboration, Noise curves used for Simulations in the update of the Observing Scenarios Paper (2020).
[72] B. P. Abbott *et al.* (KAGRA, LIGO Scientific, Virgo), Prospects for observing and localizing gravitational-wave transients with Advanced LIGO, Advanced Virgo and KAGRA, Living Rev. Rel. **19**, 1 (2016), arXiv:1304.0670 [gr-qc].
[73] L. Sun *et al.* (LIGO), LIGO A$^\sharp$: Detector Design and Science Prospects Beyond A+, (2026), arXiv:2608.11673 [astro-ph.IM].
[74] M. Maggiore *et al.* (ET), Science Case for the Einstein Telescope, JCAP **03**, 050, arXiv:1912.02622 [astro-ph.CO].
[75] M. Evans *et al.*, A Horizon Study for Cosmic Explorer: Science, Observatories, and Community, (2021), arXiv:2109.09882 [astro-ph.IM].
[76] A. G. Abac *et al.* (LIGO Scientific, VIRGO, Virgo,, KAGRA), GWTC-4.0: Population Properties of Merging Compact Binaries, Astrophys. J. Lett. **1005**, L51 (2026), arXiv:2508.18083 [astro-ph.HE].
[77] P. Auclair *et al.* (LISA Cosmology Working Group), Cosmology with the Laser Interferometer Space Antenna, Living Rev. Rel. **26**, 5 (2023), arXiv:2204.05434 [astro-ph.CO].
[78] J. C. L. Chan, E. Seo, A. K. Y. Li, H. Fong, and J. M. Ezquiaga, Detectability of lensed gravitational waves in matched-filtering searches, Phys. Rev. D **111**, 084019 (2025), arXiv:2411.13058 [gr-qc].
[79] J. C. L. Chan and E. K. Y. Li, Turning Selection Bias into a New Statistic: Asymmetry and Fringes of Lensed Gravitational Waves, (2026), arXiv:2610.18768 [gr-qc].
[80] D. Wadekar, B. Zackay, M. H.-Y. Cheung, T. Islam, J. Roulet, A. K. Mehta, T. Venumadhav, J. Mushkin, M. Zumalacarregui, and M. Zaldarriaga, Searching for lensed gravitational waves with unlensed templates, (2026), arXiv:2610.26080 [gr-qc].
[81] S. Tulin and H.-B. Yu, Dark Matter Self-interactions and Small Scale Structure, Phys. Rept. **730**, 1 (2018), arXiv:1705.02358 [hep-ph].
[82] G. P. Smith *et al.*, Multi-messenger gravitational lensing, Phil. Trans. Roy. Soc. Lond. A **383**, 20240134 (2025), arXiv:2503.19973 [astro-ph.HE].
[83] A. Mishra, A. K. Meena, A. More, S. Bose, and J. S. Bagla, Gravitational lensing of gravitational waves: effect of microlens population in lensing galaxies, Mon. Not. Roy. Astron. Soc. **508**, 4869 (2021), arXiv:2102.03946 [astro-ph.CO].
[84] X. Shan, G. Li, X. Chen, W. Zheng, and W. Zhao, Wave effect of gravitational waves intersected with a microlens field: A new algorithm and supplementary study, Sci. China Phys. Mech. Astron. **66**, 239511 (2023), arXiv:2208.13566 [astro-ph.CO].
[85] SFI, `ttps://www.sfi.org.bm/`.
[86] SF, `https://www.simonsfoundation.org/`.